Journal of Statistical Physics, Vol. 116, Nos. 1/4, August 2004 (© 2004)

Charge Stripes Due to Electron Correlations in the Two-Dimensional Spinless Falicov–Kimball Model

R. Lemański,[1] J. K. Freericks,[2] and G. Banach[3]

Received June 12, 2003; accepted October 23, 2003

We calculate the restricted phase diagram for the Falicov–Kimball model on a two-dimensional square lattice. We consider the limit where the average conduction electron density is equal to the average localized electron density, which is the limit related to the $S_z = 0$ states of the Hubbard model. After considering over 20,000 different candidate phases (with a unit cell of 16 sites or less) and their thermodynamic mixtures, we find only about 100 stable phases in the ground-state phase diagram, where the ground state is usually the phase separated mixture of two or three stable phases, that often have different electron densities than in the Maxwell-constructed mixture. We analyze these phases to describe where stripe phases occur and relate these discoveries (were appropriate) to the physics behind stripe formation in the Hubbard model.

KEY WORDS: Charge-stripes; Falicov–Kimball; Hubbard; phase-diagram.

1. INTRODUCTION

We find it fitting to write a paper on the spinless Falicov–Kimball (FK) model[(1)] to celebrate Elliott Lieb's seventieth birthday. Elliott, and his collaborators, provided two seminal results on this model: (i) the first, with Tom Kennedy, proved that there was a finite temperature phase transition to a checkerboard charge-density-wave (CDW) phase in two or more dimensions for the symmetric half-filled case,[(2, 3)] and (ii) the second, with Daniel Ueltschi and Jim Freericks, proved that the segregation principle holds for all dimensions[(4, 5)] (which states that if the total particle density is

[1] Institute of Low Temperature and Structure Research, Polish Academy of Sciences, Wrocław, Poland; e-mail: lemanski@int.pan.wroc.pl

[2] Department of Physics, Georgetown University, Washington, District of Columbia 20057; e-mail: freericks@physics.georgetown.edu

[3] Daresbury Laboratory, Cheshire WA4 4AD, Daresbury, United Kingdom.

0022-4715/04/0800-0699/0 © 2004 Plenum Publishing Corporation

less than one, then the ground state is phase separated if the interaction strength is large enough[6]). The Kennedy–Lieb result (along with an independent Brandt–Schmidt paper[7, 8]) inspired dozens of follow-up papers by researchers across the world. The Freericks–Lieb–Ueltschi paper generalized Lemberger's proof[9] from one dimension to all dimensions, which finally proved the decade old Freericks–Falicov conjecture.[6] Both papers are important, because they are the only examples where long-range order and phase separation can be proved to occur in a correlated electronic system.

The Falicov–Kimball model has an interesting history too. Leo Falicov and John Kimball invented the spin-one-half version of the model in 1969 to describe metal-insulator transitions of rare-earth compounds.[1] It turns out that John Hubbard actually "discovered" the spinless version of the FK model four years earlier in 1965,[10] when he developed the alloy-analogy solution to the Hubbard model[11] (the so-called Hubbard III solution). This latter version was rediscovered by Kennedy and Lieb in 1986[2] when they formulated it as a simple model for how crystallization can be driven by the Pauli exclusion principle.

In this contribution, we focus on another problem that can be analyzed in the FK model—the problem of stripe formation in two dimensions. The question of the relation between charge stripes, correlated electrons, and high-temperature superconductivity has been asked ever since static stripes were first seen in the nickelate[12–15] and cuprate[16–19] materials starting in 1993. Two schools of thought emerged to describe the theoretical basis for stripe formation in the Hubbard model. The Kivelson–Emery scenario[20–23] says that at large U the Hubbard model is close to a phase separation instability but the long-range Coulomb force restricts the phase separation on the nanoscale; a compromise results in static stripe-like order. The Scalapino–White scenario[24–27] says that stripes can form due to a subtle balance between kinetic-energy effects and potential-energy effects, mediated by spin fluctuations. No long range Coulomb interaction or phase separation is needed to form these stripes. There are numerous numerical studies that have tried to shed light onto this problem. Unfortunately, they have conflicting results. High temperature series expansions on the related $t-J$ model[28, 29] show that phase separation exists, but only when J is large enough, so it is not present in the large-correlation-strength limit of the Hubbard model (where $J \to 0$). Monte Carlo calculations[30–32] and exact diagonalization studies[33, 34] give different results: some calculations predict the stripe formation to occur, others show a linkage between the stripe formation and the boundary conditions selected for the problem. Mean-field-theory analyses[35, 36] seem to predict stripe formation without any phase separation. One way to make sense of these disparate results is

that both the energy of the intrinsic stripe phases and the energy for phase separation are quite close to one another, so any small change (induced by finite-size effects, statistical errors, effects of correlations not included in the perturbative expansions, or due to terms dropped or added to the Hamiltonian) can have a large effect on the phase diagram by producing a small relative change in the energetics of the different many-body states (because of their near degeneracy).

We take an alternate point of view here. We choose to examine a model that can be analyzed rigorously, and can be continuously connected to the Hubbard model. We choose the regime that connects directly with the $S_z = 0$ states of the Hubbard model. The model we analyze is the spinless Falicov–Kimball model on a square lattice

$$\mathscr{H} = -t \sum_{\langle ij \rangle} (c_i^\dagger c_j + c_j^\dagger c_i) + U \sum_{i=1}^{|\Lambda|} w_i c_i^\dagger c_i, \tag{1}$$

where $c_i^\dagger$ (c_i) creates (destroys) a spinless conduction electron at site i, t is the hopping matrix element ($\langle ij \rangle$ denotes a summation over nearest-neighbor pairs on a square lattice), $w_i = 0$ or 1 is a classical variable denoting the localized electron number at site i, and U is the on-site Coulomb interaction energy. The Fermionic operators satisfy anticommutation relations $(c_i^\dagger, c_j^\dagger)_+ = 0$, $(c_i, c_j)_+ = 0$, and $(c_i^\dagger, c_j)_+ = \delta_{ij}$. The symbol $|\Lambda|$ denotes the total number of lattice sites in the square lattice Λ. We will always be dealing with periodic configurations of localized electrons, which means we can always consider our lattice to have a large but finite number of lattice sites and periodic boundary conditions. A short presentation of these results has already appeared.[37]

The Falicov–Kimball model can be viewed as a Fermionic quantum analogue of the Ising model, while the Hubbard model can be viewed as the Fermionic quantum analogue of the Heisenberg model (indeed in the large-U limit at half filling, the Falicov–Kimball model maps onto an effective nearest-neighbor Ising model, while the Hubbard model maps onto an effective nearest-neighbor Heisenberg model). The way to link the Falicov–Kimball model to the Hubbard model is to imagine a generalization of the Hubbard model where the down-spin hopping matrix element differs from the up-spin hopping matrix element. Then as $t_\downarrow \to 0$, the down spins become heavy and are localized on the lattice; the quantum-mechanical ground state is determined by the configuration of down-spin electrons that minimizes the energy of the up-spin electrons. This is precisely the Falicov–Kimball model!

In order to maintain the connection to the Hubbard model in zero magnetic field, we must choose the average conduction electron density

$\rho_e = \sum_{i=1}^{|\Lambda|} \langle c_i^\dagger c_i \rangle / |\Lambda|$ to be equal to the average localized electron density $\rho_f = \sum_{i=1}^{|\Lambda|} w_i / |\Lambda|$, which we do here. We study the evolution from the checkerboard phase at half filling ($\rho_e = \rho_f = 1/2$) to the segregated phase, which appears when $\rho_e = \rho_f$ is small enough. Since these two phases are drastically different from each other, the transition is likely to include many different intermediate phases. Indeed, the ground state phase diagram of the Falicov–Kimball model can be quite complex. There are many different periodic phases that can be stabilized for different values of U or $\rho_e = \rho_f$. Usually the ground state ends up being a thermodynamic mixture of two or three different phases, with each phase having electron densities that differ from those of the averaged mixture. As U becomes large though, the phase diagram simplifies, as the segregated phase becomes the ground state for wider and wider ranges of the electron densities.

2. FORMALISM

Our strategy to examine the FK model is a brute-force approach which is straightforward to describe, but tedious to carry out. We employ the so-called restricted phase diagram approach, where we consider the grand-canonical thermodynamic potential of the system for all possible periodic phases of the localized electrons, selected from a finite set of candidate phases. In this work, we consider 23,755 phases, which corresponds to the set of all inequivalent phases with a unit cell that includes 16 or fewer lattice sites. In order to calculate the thermodynamic potential, we first must determine the electronic band structure for the conduction electrons for each candidate periodic phase. We employ a Brillouin-zone grid of 110×110 momentum points for each bandstructure. This requires us to diagonalize up to 16×16 matrices at each discrete momentum point in the Brillouin zone and results in at most 16 different energy bands. Hence, our calculations can be viewed as finite-size cluster calculations with cluster sizes ranging from $110 \times 110 \times 1$ up to $110 \times 110 \times 16$ depending on the number of atoms in the unit cell. An example of such a bandstructure is shown in Fig. 1. The eigenvalues of the band structure are summed to determine the ground-state energy for each number of conduction electrons. The Gibbs thermodynamic potential is then calculated for all possible values of the chemical potentials of the conduction and localized electrons through the formula

$$G(\{w_i\}) = \frac{1}{12100 N_0} \sum_{\epsilon_j < \mu_e} \epsilon_j(\{w_i\}) - \mu_e \rho_e - \mu_f \rho_f, \tag{2}$$

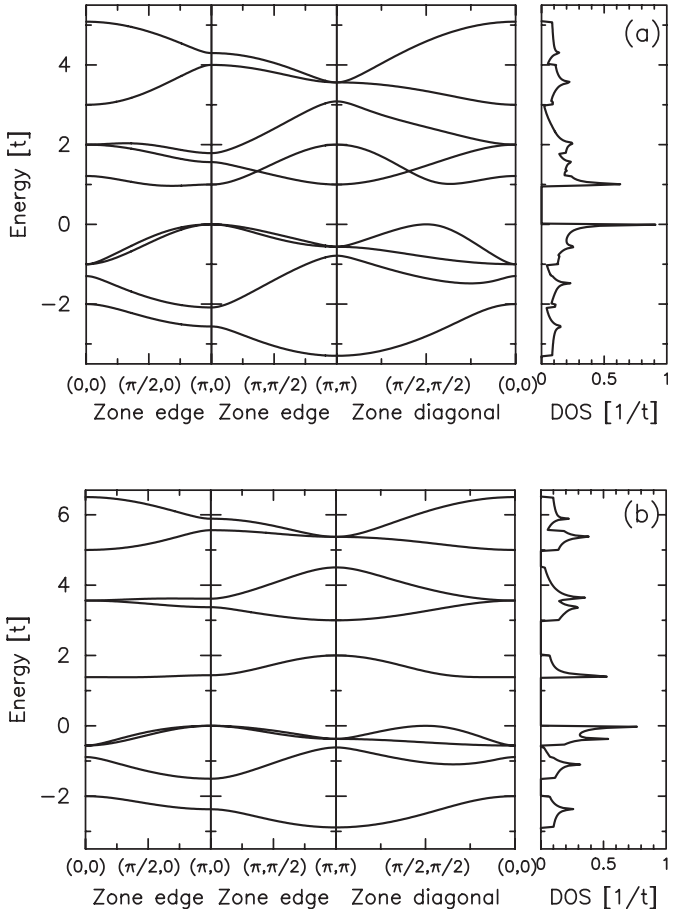

Fig. 1. Bandstructure along the irreducible wedge of the square lattice Brillouin zone for the truly two-dimensional configuration numbered 108 and depicted in Fig. 3. In panel (a) we plot the band structure and the density of states for $U = 2$. In panel (b) we show the same for $U = 4$. Note how there is less band overlap as U increases.

with μ_e and μ_f denoting the chemical potentials for the conduction and localized electrons, respectively, and N_0 denoting the number of atomic sites in the unit cell for the given configuration of localized electrons. The symbol $\epsilon_j(\{w_i\})$ denotes the energy eigenvalues of the band structure for the given configuration of localized electrons. Since the thermodynamic potential is concave, the phase diagram can be directly determined in the chemical potentials plane.[38–40] Next, we convert the grand canonical

ensemble into a canonical ensemble to determine the ground-state phase diagram as functions of ρ_e and ρ_f. We find the ground state is often a phase separated mixture of two or three different phases, which can be periodic phases, or the segregated phase. This step of the analysis is quite complicated, because small areas of stability in the grand canonical phase diagram can correspond to large regions in the canonical phase diagram, and vice versa. Finally, we restrict the analysis to the case $\rho_e = \rho_f$ and plot the phase diagram as a function of the total filling for each chosen value of U. Note that the constraint $\rho_e = \rho_f$ is for the average electron densities of the mixtures. It is often the case that the individual electron densities in a given pure phase that appears in the mixtures will not satisfy $\rho_e = \rho_f$, even though the mixture does. This computational algorithm is illustrated schematically in Fig. 2.

We find that of the initial 23,755 candidate phases, only 111 can be found in the ground-state phase diagram for the values of U that we considered. Any phase energetically excluded from appearing in the restricted phase diagram must also be excluded from the complete phase diagram. What we do not know is how our computed phase diagram will change as more candidate phases are introduced (although the majority of these additional phases also won't appear in the phase diagram).

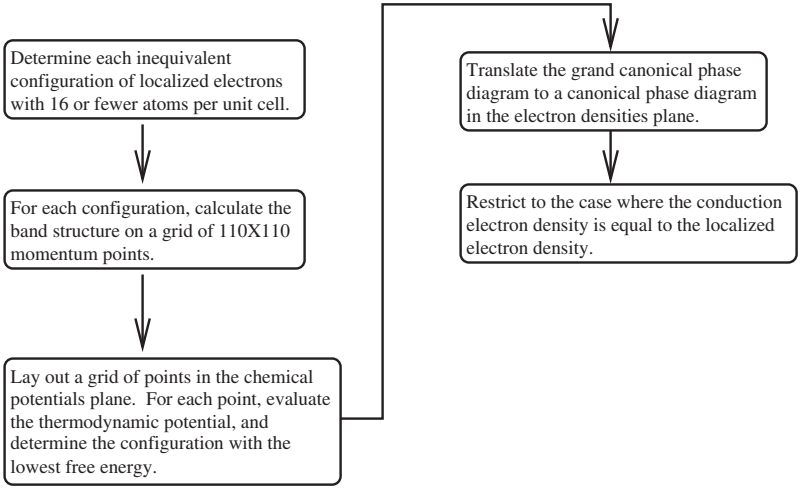

Fig. 2. Flow chart that illustrates the algorithm employed to calculate the phase diagram of the Falicov–Kimball model. Note that of the 23,755 candidate phases, only 111 appear in the restricted phase diagram.

3. RESULTS

The different phases that are stabilized in our restricted phase diagram can be grouped into different families that represent different types of geometric arrangements of the localized electrons. Unfortunately, there is no way to rigorously categorize these phases, so the grouping we have chosen arises in part from our personal taste in determining which phases appear most similar. Nevertheless, the groupings we have made are in some sense "obvious," and we believe the analysis presented here is a useful way to categorize and summarize the data. We will concentrate on describing different kinds of striped phases that are present in the phase diagram and we will motivate some of the physical principles behind their appearance in the phase diagram.

We separate the different stable phases into 10 different groups. Every stable phase is labeled by a number and depicted in Fig. 3. The small dots indicate the absence of a localized electron, while the large dots indicate the positions of the localized electrons. In the lower left corner, we shade in the unit cell of the configuration and we show with the two solid lines the translation vectors of the unit cell that allow the square lattice to be tiled by the unit cell. The different families of configurations are as follows: (i) *the empty lattice* ($\rho_e \neq 0$ and $\rho_f = 0$) denoted E which contains no localized electrons (configuration 1); (ii) *the full lattice* ($\rho_e = 0$ and $\rho_f = 1$) denoted F which contains a localized electron at each site (configuration 2); (iii) *the checkerboard phase* ($\rho_e = \rho_f = 1/2$) denoted Ch which has the localized electrons occupying the A sublattice only of the square lattice in a checkerboard arrangement (configuration 3); (iv) *diagonal non-neutral stripe phases* ($\rho_e \neq 1-\rho_f$) denoted DS which consist of diagonal checkerboard phases separated by empty diagonal stripes of slope 1 (configuration 4); (v) *axial non-neutral checkerboard stripes* ($\rho_e \neq 1-\rho_f$) denoted AChS which consist of checkerboard regions arranged in stripes oriented parallel to the x-axis and separated by empty stripes with slope 0 (configurations 5–10); (vi) *diagonal neutral stripe phases* ($\rho_e = 1-\rho_f$) denoted DNS which consist of localized electrons arranged in the checkerboard phase and separated by fully occupied striped regions of slope 1, or equivalently, checkerboard phases with diagonal antiphase boundaries (configurations 11–19); (vii) *axial non-neutral stripe phases* ($\rho_e \neq 1-\rho_f$) denoted AS which consist of fully occupied vertical (or horizontal) stripes separated by empty stripes, which are translationally invariant in the vertical (or horizontal) direction (configurations 20–54); (viii) *neutral phases* ($\rho_e = 1-\rho_f$) denoted N which consist of neutral phases in an arrangement that does not look like any simple stripe phase (some neutral phases can be described in a stripe picture, such as configuration 61 which has a slope

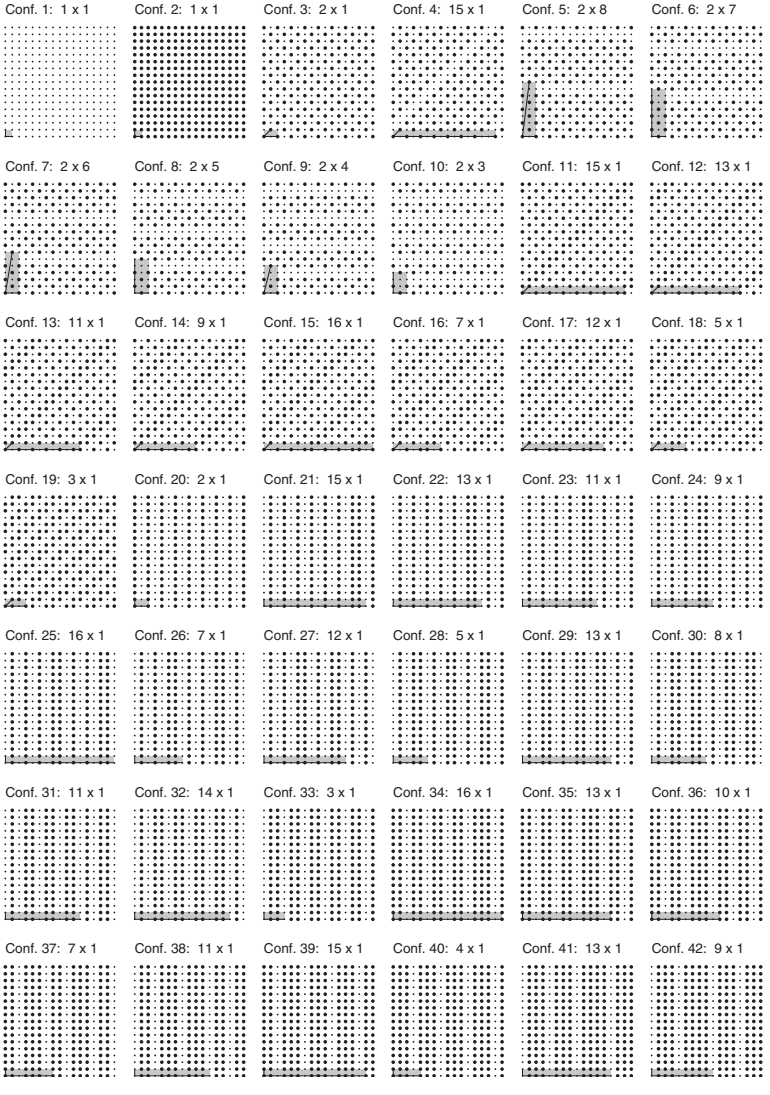

Fig. 3. Picture of the configurations of the localized electrons that appear in the restricted phase diagram. The large dots refer to sites occupied by localized electrons, and the small circles denote empty sites. The shaded region in the lower left corner shows the unit cell, and the line segments show the translation vectors that are used to tile the two dimensional plane. Each of the 111 configurations is assigned a number and we also note the size and shape of the unit cell above each panel.

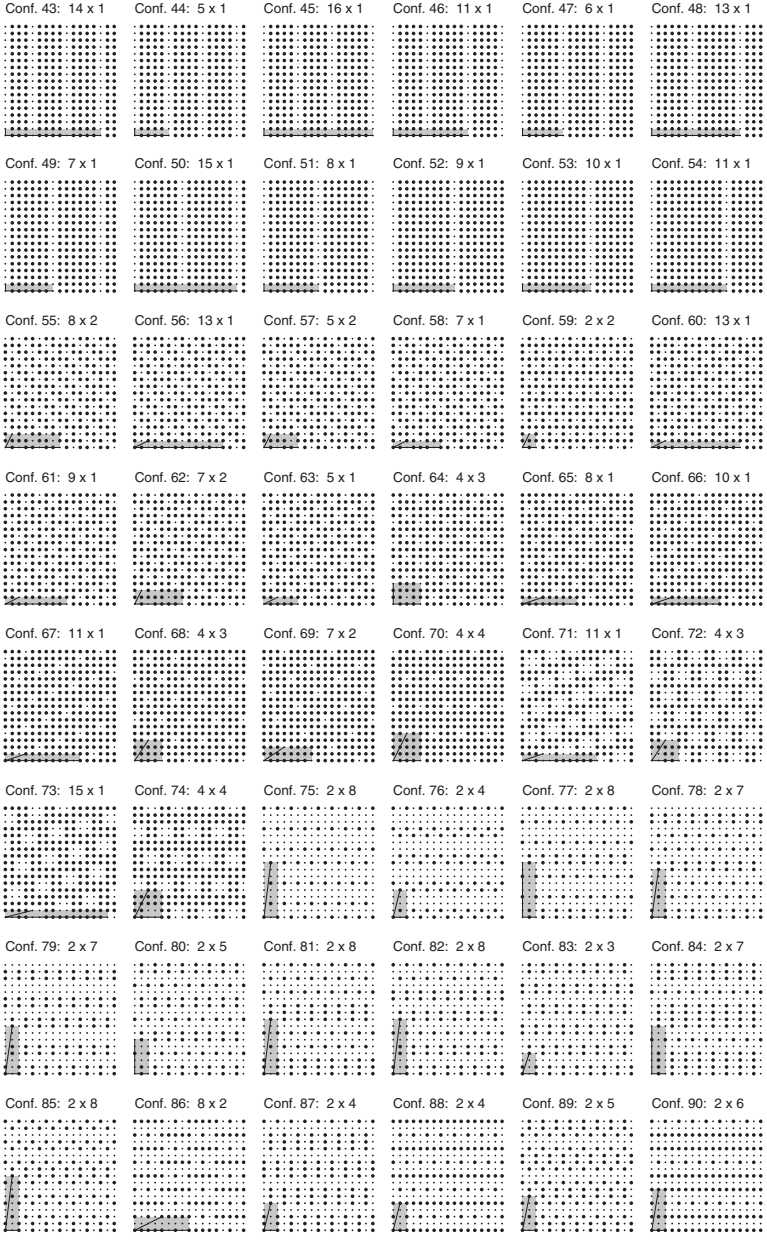

Fig. 3. Continued.

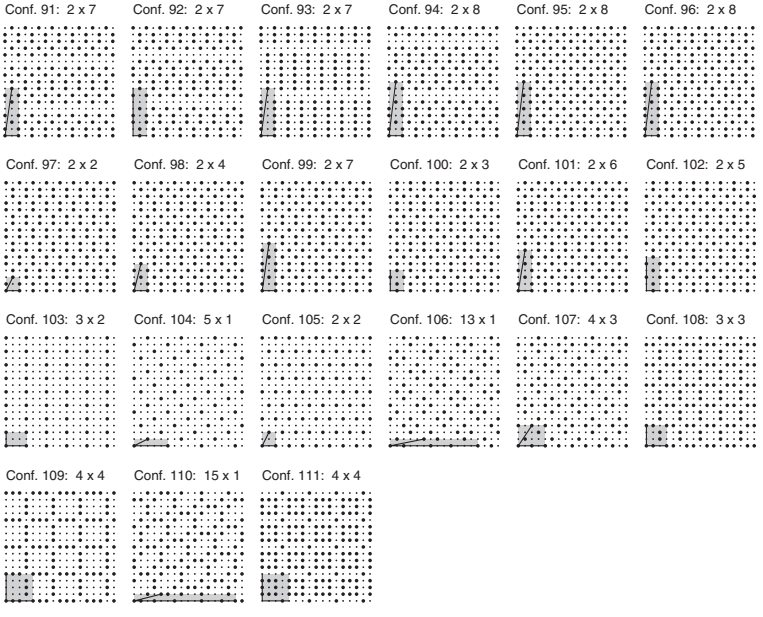

Fig. 3. Continued.

1/3 empty lattice stripe, but we prefer to refer to them as non-stripe phases) (configurations 55–70); (ix) *four-molecule phases* ($\rho_e \neq 1-\rho_f$) denoted 4M which can be described as a "bound" four-molecule square of empty sites tiled inside an occupied lattice framework (configurations 71–74); (x) *two-dimensional non-neutral phases* ($\rho_e \neq 1-\rho_f$) denoted 2D which consist of phases with the localized electrons arranged in a fashion that is not stripe-like and requires a two-dimensional unit cell to describe them (once again, some phases like configuration 75 could be described as a slope 3/2 stripe, but appears to us more like a 2D phase) (configurations 75–111). Note that our usage of the term neutral may not seem natural, but it arises from the fact that a partial particle-hole transformation[2] (of either the conduction or the localized electrons) will change $U \to -U$ and will change the filling of the transformed electrons from $\rho \to 1-\rho$, resulting in a neutral arrangement of particles for the attractive Falicov–Kimball model. Hence the phases with $\rho_e + \rho_f = 1$ in the repulsive case are connected to these so-called neutral phases, so we use that nomenclature for the repulsive case as well.

Generically, we find the canonical phase diagram does not contain pure phases from one of the 111 stable phases, but rather forms mixtures of

Table I. Summary of the Stability of Different Phases for the Five Different Values of U Where We Performed Calculations (1, 2, 4, 6, and 8). Each Column Shows the Phases that Appear in the Phase Diagram for a Given Value of U. The Numbers Correspond to the Labels in Fig. 3

Phase category	$U=1$	$U=2$	$U=4$	$U=6$	$U=8$
E	1	1	1	1	1
F	2	2	2	2	2
Ch	3	3	3	3	3
DS	4				
AChS	5–10				
DNS		11–14			14–19
AS	20, 26–33	20, 28–40	20–54	33–52	
N			59	59–64	55–70
4M	71–73	73–74			
2D	75–78, 80–82 84–92, 94–100, 103–107	79, 82–83, 87–88, 93, 98–102, 105–106 110–111	83, 108–109	108	

two or three periodic phases, or one or two periodic phases and the empty lattice (which is often needed to get the average conduction-electron filling correct in the mixture). When we are doped sufficiently far from half filling, we are in the segregated phase, which is a mixture of the E and F phases. We consider 5 different values of U in our computations: $U=1$, 2, 4, 6, and 8. The phase diagram is quite complex, with many of the different 111 phases appearing for different values of U. We summarize which phases appear in Table I.

We begin our discussion with the weak-coupling value $U=1$ where 50 phases appear. The phase diagram is summarized in Fig. 4. We use a solid line to indicate the region of the particle density where a particular phase appears in the ground state (either as a pure phase or as a mixture). The phases that appear in a mixture at a given density are found by determining the solid vertical lines that intersect a horizontal line drawn to pass through the given particle density. The phase diagram has shading included to separate the regions of the different categories of phases. The numeric labels are shown to make it easier to determine the actual phases present in the diagram. We plot similar phase diagrams for $U=2$ (38 phases), 4 (42 phases), 6 (30 phases), and 8 (25 phases) in Figs. 5–8, respectively. A schematic phase diagram that illustrates the generic features of the phase diagram in the electron density, interaction-strength plane appears in Fig. 9.

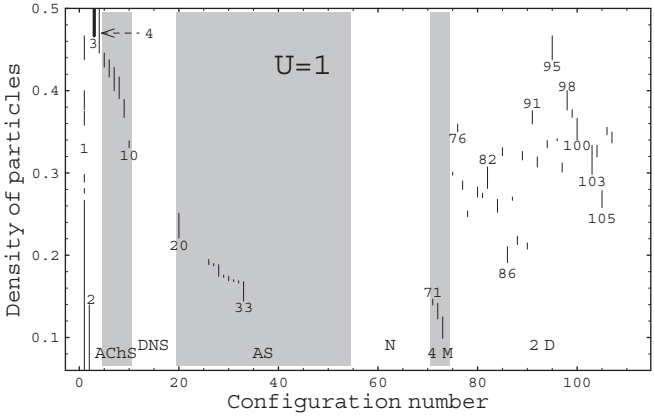

Fig. 4. Phase diagram for $U = 1$. The solid lines show the regions of electron density where a particular phase appears (either as a single phase or as a mixture). The horizontal axis labels the different configurations that are present, and the shading helps to distinguish the different categories of the phases. The numbers are included as a guide to make it easier to identify the different stable phases in the diagram.

As can be seen from these figures, the generic phase diagram is quite complex, and by looking at the different phases in Fig. 3, many of the phases have stripe-like structures to them. To begin our discussion of these results, we must first recall the rigorous results known for this model. When $\rho_e = \rho_f = 1/2$, the ground state is the checkerboard phase (configuration 3) for all U. This can be seen in all of the phase diagrams

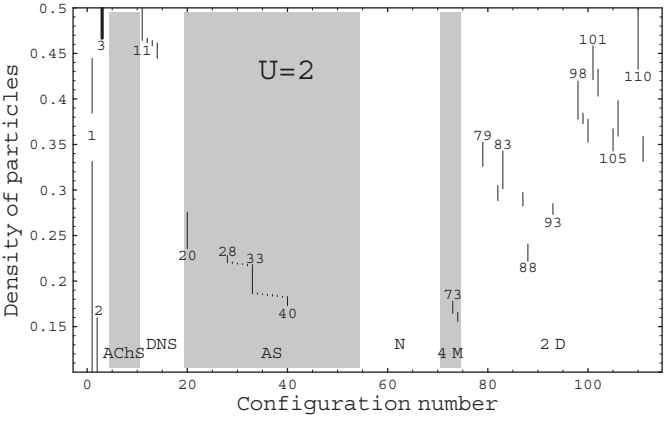

Fig. 5. Phase diagram for $U = 2$. The notation is the same as in Fig. 4.

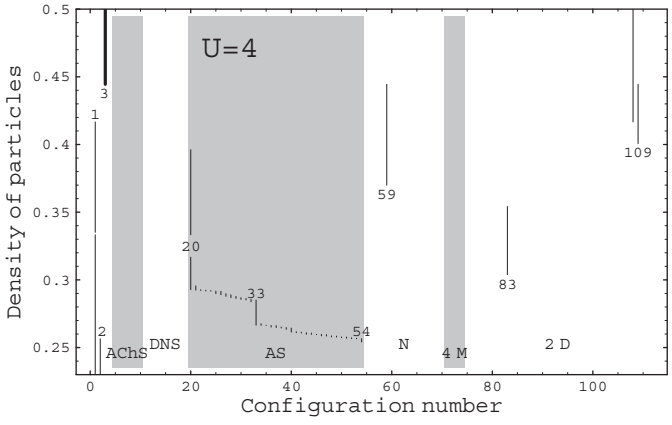

Fig. 6. Phase diagram for $U = 4$. The notation is the same as in Fig. 4.

plotted. When $\rho_e = \rho_f \neq 1/2$, the ground state becomes the phase separated segregated phase when U is large enough. So there is a simplification in the phase diagram as we increase U, and the most complex phase diagram appears in the $U \to 0$ limit. That limit is also the most difficult computationally, because the differences in the energies between different configurations also becomes small for small U, and the numerical accuracy must be huge in order to achieve trustworthy results. This is why we do not report any phase diagrams with $U < 1$ here.

Looking at the $U = 8$ case shown in Fig. 8, we see that as we move away from half filling, we initially find mixtures between the checkerboard

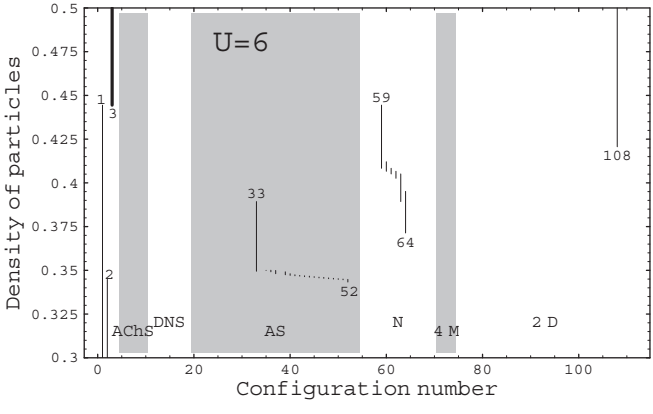

Fig. 7. Phase diagram for $U = 6$. The notation is the same as in Fig. 4.

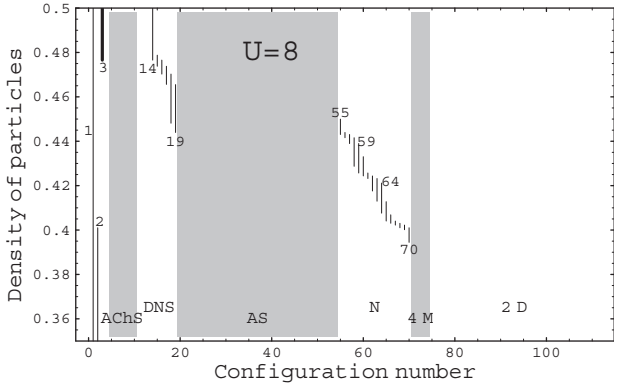

Fig. 8. Phase diagram for $U = 8$. The notation is the same as in Fig. 4.

phase, other diagonal stripe phases, and the empty lattice. When we examine the structure factors associated with the diagonal stripe phases, we find that they tend to have more weight along the Brillouin zone diagonal than elsewhere. Hence, these diagonal stripe phases are being stabilized by a "near-nesting" instability of the noninteracting Fermi surface, and the

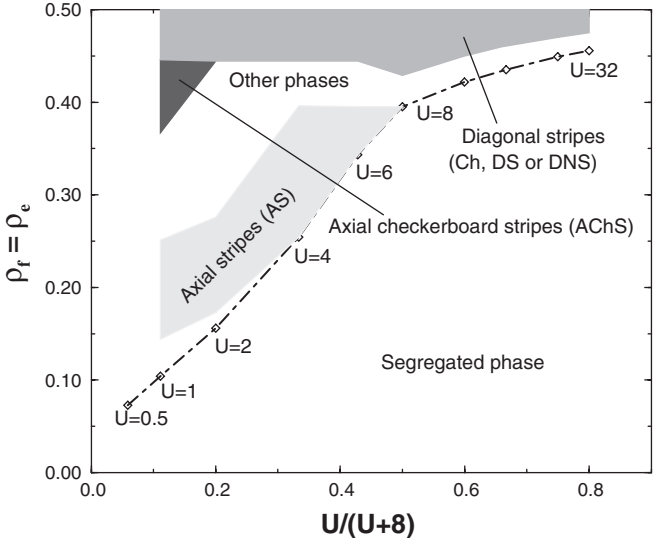

Fig. 9. Schematic phase diagram which indicates the different categories of phases that appear in the restricted phase diagram.

overall mixtures are required to maintain the average fillings of the conduction and localized electrons. As we move farther from half filling, the checkerboard phase disappears from the mixtures, and then a series of neutral phases enter the mix which retain some appearance of diagonal stripes, but with more and more "defects" to the stripes that make them look more two-dimensional. We find the localized electron density of these phases increases as we reduce the total filling, which is what we expect as we move toward the segregated phase which involves a mixture of the E and F configurations. Note that the formation of many different stripe phases, occurs without needing the long-range Coulomb interaction to oppose the tendency towards phase separation, when we are close to half filling. Indeed, the ground state is often a phase separated mixture, but it is a mixture of stripe-like phases, which occur automatically, without the need to add any other physics to the system. This regime, is the closest to the Kivelson–Emery picture, but we see it has more complex behavior than what they envisioned when they examined the Hubbard model.

Moving on to the $U = 6$ case in Fig. 7, we find a significant change in the phase diagram. The grouping of diagonal stripes near half filling disappears and we instead find the ground state to initially be a mixture between the checkerboard phase, a truly two-dimensional screen-like phase (configuration 108) and the empty lattice. Here, if we include a long-range Coulomb interaction, we would likely form diagonal stripes, but the mixture would be more complicated because it would include this screen-like structure as well. As we dope further away, we see a smaller number of the neutral phases, which look somewhat like diagonal stripes with a large number of defects in them, and then we go to a very different class of mixtures, dominated by the presence of the axial stripe phase in configuration 33. As that phase becomes destabilized, we find a cascade of many other axial stripes entering, before the segregated phase takes over. This transition from diagonal stripes to axial stripes as a function of the electron filling, also occurs because of a "near-nesting" effect. The structure factors of the axial stripe phases are peaked predominantly along the zone edge, and as we dope further from half filling, this is where nesting is more likely to occur. The cascade of stable phases that enter after configuration 33 is destabilized, have a progression of the peaks in their structure factor moving towards the zone center, which is also expected, since they are progressively heading towards the segregated phase. A similar kind of transition from diagonal stripes to axial stripes is seen in the Hubbard model studies, with the critical density lying near 0.375, as we see here too.

By the time we decrease to $U = 4$ shown in Fig. 6, we find even more interesting behavior. Now, when we are near half filling, we find two more

configurations, a nonneutral phase (configuration 59) and a two-dimensional phase (configuration 109) joining with the checkerboard phase and configuration 108 in the initial mixtures. Each of these phases looks like a "square-lattice screen" with differing size "holes" in the screen. These two-dimensional structures are not stripe-like and it would be interesting to see if they could appear in the Hubbard model. As we dope further away, we enter the axial stripe region, now dominated by configuration 20 first, then there is a cascade to configuration 33, then a cascade to the segregated phase. This value of U is a truly intermediate value, where many different mechanisms for ordering are present and the system can change very rapidly in response to a modification in the density.

As $U = 2$ (Fig. 5), we see more modifications in the phase diagram. Now we see other diagonal stripe phases mixing with the checkerboard phase near half filling. This region would correspond to the Scalapino–White regime, where the stripe formation is driven more by interplays between the kinetic and potential energies and nesting effects (driven by charge fluctuations in the FK model and spin fluctuations in the Hubbard model). In addition, a much larger number of the 2D phases enter also close to half filling, illustrating the prevalence of these "screen-like" phases as well. The axial stripes also enter as we dope further away from half filling, but the configurations 20 and 33 are not nearly as stable as they are for slightly larger U. Here, we see the four-molecule phases being stabilized just before the system phase separates into the segregated phase.

Finally, for $U = 1$, shown in Fig. 4, the predominance of the diagonal stripes, near half filling increases now supplemented by the axial checkerboard stripes, but then there is a plethora of different 2D phases that also enter as the system is doped somewhat farther from half filling, then we see a similar evolution, first to AS and then to 4M phases before the segregated phase. Here there is a tremendous complexity to the phase diagram, with many different mixtures being present due to the competition between kinetic energy and potential energy minimization brought about by the many-body aspects of the problem.

The general picture, illustrated schematically in Fig. 9, now emerges: near half filling, we often find diagonal stripes and screen-like two-dimensional phases, then a rapid transition to the segregated phase for large U. As U is reduced, we can dope farther away from half filling before segregating, which allows many other phases to enter. In particular, there is a large region of stability for axial stripes, and as U is reduced further, we see the emergence of axial checkerboard stripes close to half filling, near the diagonal stripes, and four-molecule phases appearing near the segregation boundary.

4. CONCLUSIONS

In this manuscript we have numerically studied how the FK model makes the transition from the checkerboard phase at half filling to the segregated phase as the density is lowered. Since these two phases are very different from one another, there are many different pathways that one might imagine the system to take in making this crossover. Indeed we find that the pathway varies dramatically as a function of U. For large U, we have a relatively simple transition between diagonal stripe-like phases which become more two-dimensional as the localized electron density increases, until the system gives way to the segregated phase. As U is lowered, we first see two-dimensional-"screen"-like phases enter, then we see axial stripes emerge, followed by four-molecule phases and axial checkerboard stripes. The complexity of the phase diagram greatly increases as the interaction strength decreases.

It is interesting to ask how we might expect these results to change if we allowed more configurations into our restricted phase diagram. We don't know this answer in particular, but we do know, that as we increase the size of the unit cells that are considered in the restricted phase diagram, the *percentage of phases that enter into the phase diagram decreases as the unit cell size increases*. For example, of the 23,755 candidate phases only a small fraction (111 or 0.5%) appear in the phase diagram. While the number of phases appearing in the complete (unrestricted) phase diagram is probably infinite, it is also likely that they correspond to a relatively small fraction of all of the possible candidate states, and hence we don't expect dramatic changes to the phase diagram as more candidate phases are considered. We can illustrate this point in more detail by comparing three interrelated phases, such as phases 31, 32, and 33. Note how phase 32 is a higher-period phase composed of the unit cells of phases 31 and 33. In a restricted phase diagram that has a maximal period small enough that phase 32 is not considered, we find a mixture of phases 31 and 33 to appear. As we increase the maximal period, we find phase 32 enters, but it does not remove phases 31 or 33 from the phase diagram (in fact, phase 33 is particularly stable and occupies a large region of phase space for some diagrams). Hence, we conjecture that the generic picture for additional phases to enter into the phase diagram will be phases closely related to the current phase mixtures, and which will, in most likelihood, occupy relatively small regions of the phase diagram. Of course, exceptions to this picture can occur, and are difficult to predict.

Another interesting question to ask is how do these results for the FK model shed light on the stripe-formation problem in the Hubbard model. By continuity, we expect these results not to change too dramatically as we

turn on a small hopping for the localized electrons (although now we must summarize our results in terms of correlation functions for the two kinds of electrons, since both are now mobile). But we also know for many fillings, there will be a "phase transition" as a function of the hopping, since the ground state of the Hubbard model is not ferromagnetic for all fillings and large U (which is what the segregated phase maps to in the Hubbard model). The results are likely to be closer to what happens in the Hubbard model close to half filling, because the analogue of the antiferromagnetic phase is the checkerboard phase, and that is present for all U in the Hubbard model at $T = 0$. In general, we also feel that the FK model phase diagram must be more complicated than the Hubbard model phase diagram because of the mobility of both electrons in the latter. We feel one of the most important results of this work is that there may be two-dimensional phases that are not stripe like that form ground-state configurations for some values of the filling in the Hubbard model, and such configurations will be worthwhile to investigate with the numerical techniques that currently exist.

In conclusion, we are delighted to be able to shed some light on the interesting question for the FK model of how one makes a transition from the checkerboard phase at half filling to the segregated phase away from half filling. Since Elliott Lieb has had an important impact in proving the stabilization of these two phases, we find it fitting to ask the questions about how the two phases inter-relate. Perhaps these numerical calculations can further inspire new rigorous work that helps to identify the pathway between these two phases.

ACKNOWLEDGMENTS

R.L. and G.B. acknowledge support from the Polish State Committee for Scientific Research (KBN) under Grant No. 2P03B 131 19 and J.K.F. acknowledges support from the NSF under Grant No. DMR-0210717. We also acknowledge support from Georgetown University for a travel grant in the fall of 2001.

REFERENCES

1. L. M. Falicov and J. C. Kimball, Simple model for semiconductor-metal transitions: SmB_6 and transition-metal oxides, *Phys. Rev. Lett.* **22**:997–1000 (1969).
2. T. Kennedy and E. H. Lieb, An itinerant electron model with crystalline or magnetic long range order, *Physica A* **138**:320–358 (1986).
3. E. H. Lieb, A model for crystallization: A variation on the Hubbard model, *Physica A* **140**:240–250 (1986).
4. J. K. Freericks, E. H. Lieb, and D. Ueltschi, Phase separation due to quantum mechanical correlations, *Phys. Rev. Lett.* **88**:106401–1-4 (2002).

5. J. K. Freericks, E. H. Lieb, and D. Ueltschi, Segregation in the Falicov–Kimball model, *Comm. Math. Phys.* **227**:243–279 (2002).
6. J. K. Freericks and L. M. Falicov, Two-state one-dimensional spinless Fermi gas, *Phys. Rev. B* **41**:2163–2172 (1990).
7. U. Brandt and R. Schmidt, Exact results for the distribution of f-level ground state occupation in the spinless Falicov–Kimball model, *Z. Phys. B* **63**:45–53 (1986).
8. U. Brandt and R. Schmidt, Ground state properties of a spinless Falicov–Kimball model; Additional features, *Z. Phys. B* **67**:43–51 (1987).
9. P. Lemberger, Segregation in the Falicov–Kimball model, *J. Phys. A* **25**:715–733 (1992).
10. J. Hubbard, Electron correlations in narrow energy bands III. An improved solution, *Proc. Roy. Soc. (London) A* **281**:401–419 (1965).
11. J. Hubbard, Electron correlations in narrow energy bands, *Proc. Roy. Soc. (London) A* **276**:238–257 (1963).
12. C. H. Chen, S.-W. Cheong, and A. S. Cooper, Charge modulations in $La_{2-x}Sr_xNiO_{4+y}$: Ordering of polarons, *Phys. Rev. Lett.* **71**:2461–2464 (1993).
13. J. M. Tranquada, D. J. Buttrey, V. Sachan, and J. E. Lorenzo, Simultaneous ordering of holes and spins in $La_2NiO_{4.125}$, *Phys. Rev. Lett.* **73**:1003–1006 (1994).
14. V. Sachan, D. J. Buttrey, J. M. Tranquada, J. E. Lorenzo, and G. Shirane, Charge and spin ordering in $La_{2-x}Sr_xNiO_{4.00}$ with $x = 0.135$ and 0.20, *Phys. Rev. B* **51**:12742–12746(1995).
15. J. M. Tranquada, J. E. Lorenzo, D. J. Buttrey, and V. Sachan, Cooperative ordering of holes and spins in $La_2NiO_{4.125}$, *Phys. Rev. B* **52**:3581–3595 (1995).
16. J. M. Tranquada, B. J. Sternlieb, J. D. Axe, Y. Nakamura, and S. Uchida, Evidence for stripe correlations of spins and holes in copper oxide superconductors, *Nature (London)* **375**:561–563 (1995).
17. J. M. Tranquada, J. D. Axe, N. I. Y. Nakamura, S. Uchida, and B. Nachumi, Neutron-scattering study of stripe-phase order of holes and spins in $La_{1.48}Nd_{0.4}Sr_{0.12}CuO_4$, *Phys. Rev. B* **54**:7489–7499 (1996).
18. J. M. Tranquada, J. D. Axe, N. Ichikawa, A. R. Moodenbaugh, Y. Nakamura, and S. Uchida, Coexistence of, and competition between, superconductivity and charge-stripe order in $La_{1.6-x}Nd_{0.4}Sr_xCuO_4$, *Phys. Rev. Lett.* **78**:338–341 (1997).
19. H. A. Mook, P. Dai, and F. Doğan, Charge and Spin Structure in $YBa_2Cu_3O_{6.35}$, *Phys. Rev. Lett.* **88**:097004–1-4 (2002).
20. V. J. Emery, S. A. Kivelson, and H. Q. Lin, Phase separation in the $t-J$ model, *Phys. Rev. Lett.* **64**, 475–478 (1990).
21. E. W. Carlson, S. A. Kivelson, Z. Nussinov, and V. J. Emery, Doped Antiferromagnets in High Dimension, *Phys. Rev. B* **57**:14704–14721 (1998).
22. L. P. Pryadko, S. A. Kivelson, and D. W. Hone, Instability of charge ordered states in doped antiferromagnets, *Phys. Rev. Lett.* **80**:5651–5654 (1998).
23. L. P. Pryadko, S. A. Kivelson, V. J. Emery, Y. B. Bazaliy, and E. A. Demler, Topological doping and the stability of stripe phases, *Phys. Rev. B* **60**:7541–7557 (1999).
24. S. R. White and D. J. Scalapino, Density matrix renormalization group study of the striped phase in the 2D $t-J$ Model, *Phys. Rev. Lett.* **80**:1272–1275 (1998).
25. S. R. White and D. J. Scalapino, Energetics of domain walls in the 2D $t-J$ model, *Phys. Rev. Lett.* **81**:3227–3230 (1998).
26. S. R. White and D. J. Scalapino, Competition between stripes and pairing in a $t-t'-J$ model, *Phys. Rev. B* **60**:R753–R756 (1999).
27. S. R. White and D. J. Scalapino, Phase separation and stripe formation in the two-dimensional $t-J$ model: A comparison of numerical results, *Phys. Rev. B* **61**:6320–6326 (2000).

28. W. O. Putikka, M. U. Luchini, and T. M. Rice, Aspects of the phase diagram of the two-dimensional $t-J$ model, *Phys. Rev. Lett.* **68**:538–541 (1992).
29. W. O. Putikka and M. U. Luchini, Limits on phase separation for two-dimensional strongly correlated electrons, *Phys. Rev. B* **62**:1684–1687 (2000).
30. A. C. Cosentini, M. Capone, L. Guidoni, and G. B. Bachelet, Phase separation in the two-dimensional Hubbard model: A fixed-node quantum Monte Carlo study, *Phys. Rev. B* **58**:R14685–R14688 (1998).
31. M. Calandra, F. Becca, and S. Sorella, Charge fluctuations close to phase separation in the two-dimensional $t-J$ model, *Phys. Rev. Lett.* **81**:5185–5188 (1998).
32. C. S. Hellberg and E. Manousakis, Green's-function Monte Carlo for lattice fermions: Application to the $t-J$ model, *Phys. Rev. B* **61**:11787–11806 (2000).
33. E. Dagotto, Correlated electrons in high-temperature superconductors, *Rev. Mod. Phys.* **66**:763–840 (1994).
34. C. S. Hellberg and E. Manousakis, Stripes and the $t-J$ Model, *Phys. Rev. Lett.* **83**:132–135 (1999).
35. J. Zaanen and A. M. Oleś, Striped phase in the cuprates as a semiclassical phenomenon, *Ann. Phys. (Leipzig)* **5**:224–246 (1996).
36. D. Góra, K. Rosciszewski, and A. M. Oleś, Electron correlations in stripe phases for doped antiferromagnets, *Phys. Rev. B* **60**:7429–7439 (1999).
37. R. Lemański, J. K. Freericks, and G. Banach, Stripe phases in the two-dimensional Falicov–Kimball model, *Phys. Rev. Lett.* **89**, 196403–1-4 (2002).
38. G. I. Watson and R. Lemański, The ground-state phase diagram of the two-dimensional Falicov–Kimball model, *J. Phys. Conden. Matter* **7**:9521–9542 (1995).
39. Z. Gajek, J. Jędrzejewski, and R. Lemański, Canonical phase diagrams of the 1D Falicov–Kimball model at $T = 0$, *Physica A* **223**:175–192 (1996).
40. Z. Gajek, J. Jędrzejewski, and R. Lemański, New phases and structural phase transitions in the 1D Falicov–Kimball model at $T = 0$, *Phase Transitions* **57**:139–151(1996).